Published in final edited form as:
*Toxicology*. 2013 September 15; 311(3): . doi:10.1016/j.tox.2013.06.013.

# Absence of a p53 allele delays nitrogen mustard-induced early apoptosis and inflammation of murine skin

**Swetha Inturi**[a], **Neera Tewari-Singh**[a], **Anil K. Jain**[a], **Srirupa Roy**[a,#], **Carl W. White**[b], and **Rajesh Agarwal**[a,*]

Swetha Inturi: Swetha.Inturi@ucdenver.edu; Neera Tewari-Singh: Neera.Tewari-Singh@ucdenver.edu; Anil K. Jain: Anil.Jain@ucdenver.edu; Srirupa Roy: Srirupa.Roy@ucsf.edu; Carl W. White: Carl.W.White@ucdenver.edu

[a]Department of Pharmaceutical Sciences, University of Colorado Skaggs School of Pharmacy and Pharmaceutical Sciences, 12850 E. Montview Blvd, Aurora, CO 80045, USA

[b]Department of Pediatrics, University of Colorado Denver, 12850 E. Montview Blvd, Aurora, CO 80045, USA

## Abstract

Bifunctional alkylating agent sulfur mustard (SM) and its analog nitrogen mustard (NM) cause DNA damage leading to cell death, and potentially activating inflammation. Transcription factor p53 plays a critical role in DNA damage by regulating cell cycle progression and apoptosis. Earlier studies by our laboratory demonstrated phosphorylation of p53 at Ser15 and an increase in total p53 in epidermal cells both in vitro and in vivo following NM exposure. To elucidate the role of p53 in NM-induced skin toxicity, we employed SKH-1 hairless mice harboring wild type (WT) or heterozygous p53 (p53+/−). Exposure to NM (3.2 mg) caused a more profound increase in epidermal thickness and apoptotic cell death in WT relative to p53+/− mice at 24 h. However, by 72 h after exposure, there was a comparable increase in NM-induced epidermal cell death in both WT and p53+/− mice. Myeloperoxidase activity data showed that neutrophil infiltration was strongly enhanced in NM-exposed WT mice at 24 h persisting through 72 h of exposure. Conversely, robust NM-induced neutrophil infiltration (comparable to WT mice) was seen only at 72 h after exposure in p53+/− mice. Similarly, NM-exposure strongly induced macrophage and mast cell infiltration in WT, but not p53+/− mice. Together, these data indicate that early apoptosis and inflammation induced by NM in mouse skin are p53-dependent. Thus, targeting this pathway could be a novel strategy for developing countermeasures against vesicants-induced skin injury.

### Keywords

Sulfur mustard; nitrogen mustard; skin p53; skin inflammation; skin apoptosis



[*]**Corresponding author: Rajesh Agarwal**, Department of Pharmaceutical Sciences, University of Colorado Denver School of Pharmacy, 12850 E. Montview Blvd, Room V20- 2118, Box C238, Aurora, CO 80045, USA, Phone: 303-724-4055, Fax: 303-724-7266. Rajesh.Agarwal@ucdenver.edu.
[#]Department of Pathology, University of California San Francisco, San Francisco, CA, USA



**Conflict of Interest Statements:** The authors declare that there are no conflicts of interest.

## 1. Introduction

Nitrogen mustard (NM), a structural analog of warfare agent sulfur mustard (SM), belongs to the class of chemical vesicants which cause blistering of skin and damage to mucus membranes (Atkinson 1947; Ghanei et al. 2010). Exposure to mustards occurs through skin and/or respiration, and these agents rapidly penetrate epithelial tissues due to their lipophilic nature (Chilcott et al. 2000; Kumar et al. 2010). The primary targets of mustards are the skin, eyes and respiratory tissues, and depending on the extent and duration of exposure, they may also damage the gastrointestinal tract and bone marrow, leading to development of various malignancies (Kehe et al. 2008). The clinical symptoms of SM exposure begin to appear on skin within one to several hours after exposure. These include itching, burning, erythema and blister formation (Le and Knudsen 2006; Newmark et al. 2007; Papirmeister et al. 1984; Shakarjian et al. 2010). Due to structural similarities with SM, exposure to NM also causes similar clinical pathologies (Sharma et al. 2008).

Toxic effects of mustard agents are attributed to their alkylating nature, specifically causing DNA damage (Guainazzi et al. 2010; Rutman et al. 1969; Shukla et al. 2007). If DNA damage is not repaired in a timely manner, this could lead to cell death or mutations (Kehe et al. 2008). These agents also induce oxidative stress through depletion of intracellular glutathione (GSH), resulting in oxidative stress, followed by oxidative DNA damage, lipid peroxidation and protein oxidation (Dirven et al. 1996; Paromov et al. 2007). The DNA-damaged cells undergo activation of various signaling pathways, such as poly (ADP-ribose) polymerase (PARP), ataxia telangiectasia mutated (ATM), ataxia telangiectasia-Rad3-related (ATR), p53 and NF-κB, which play an important role in DNA damage repair, cell cycle arrest, and/or inflammation (Basu et al. 2000; Lavin and Kozlov 2007). P53, regarded as the ‘guardian of the genome’, maintains genomic stability through cell cycle arrest in order to allow cells to repair damaged DNA. Alternatively, it promotes apoptotic cell death to remove excessively damaged cells and limit genotoxic insult (Ikehata et al. 2010; Lane 1992). In recent studies, SM, NM and 2-chloroethyl ethyl sulfide (CEES, a monofunctional analog of SM) have been shown to increase p53 phosphorylation at Ser15 and total p53 levels (Inturi et al. 2011; Jowsey et al. 2012; Minsavage and Dillman 2007; Tewari-Singh et al. 2012). Our studies employing mouse epidermal keratinocytes demonstrated that NM exposure caused S-phase arrest and that CEES exposure increased apoptosis in SKH-1 hairless mouse skin (Jain et al. 2011b; Tewari-Singh et al. 2009). Notably, toxic effects of mustards are mediated by p53 via transcriptional activation of various molecules (p21, Bax, PUMA, Noxa, etc.) (Haupt et al. 2003).

Studies focusing on the effects of p53 on inflammation and apoptosis have shown that p53 null/heterozygous mice were more susceptible to DNA damaging agents and related skin toxicity and inflammation, with compromised ability of mice to properly respond to genotoxic insults (Boley et al. 2002; Tavana et al. 2010). Similarly, p53-deficient or heterozygous mouse embryonic fibroblasts are more sensitive to NM-induced DNA damage and cytotoxicity (Hawkins et al. 1996). Conversely, sustained activation of p53 following DNA damage caused increased apoptotic cell death leading to pro-tumorigenic inflammation (Yan et al. 2012). Importantly, cell death by itself could activate the innate immune response leading to increased inflammation (Basu et al. 2000; Kono and Rock 2008; Rock and Kono 2008; Shi et al. 2000). Considering the significant role of p53 in DNA damage response and inflammation, and that p53 is activated in response to NM-induced DNA damage, we investigated, for the first time, the role of p53 in NM-induced skin injury employing a genetic approach. SKH-1 hairless mice are widely used as an in vivo model for study of dermal toxicants as well as DNA damaging agents, including mustards and ultraviolet irradiation (Gu et al. 2007; Jain et al. 2011a; Joseph et al. 2011; Tewari-Singh et al. 2012; Tewari-Singh et al. 2009). Consequently, employing p53 wild type (WT) and p53

heterozygous (p53+/−) SKH-1 hairless mice, we examined the effect of p53 deficiency on NM-induced skin damage, cell death and inflammation. Our data suggest that NM-induced early apoptosis and inflammation are mediated by p53, and that apoptotic cell death might also play a key role in the early inflammation caused by NM exposure.

## 2. Materials and methods

### 2.1 Materials

DeadEnd™ Colorimetric TUNEL (TdT-mediated dUTP Nick-End Labeling) System was from Promega (Madison, WI). Fluoro MPO™ Fluorescent Myeloperoxidase (MPO) Detection Kit was from Cell Technology (Mountain View, CA). BM8 monoclonal F4/80 rat anti-mouse IgG2a antibody was from Caltag labs (Invitrogen, Carlsbad, CA). NM (mechlorethamine hydrochloride; 98%), Toluidine blue and other chemicals used were purchased from Sigma-Aldrich Chemicals Co. (St. Louis, MO) unless otherwise specified.

### 2.2 Animal, treatments, and tissue collection

SKH-1 hairless p53+/− mice were previously generated in our laboratory by breeding p53−/− C57Bl/6 mice (The Jackson Laboratory, Bar Harbor, Maine) with WT SKH-1 hairless mice (Charles River Laboratories, Wilmington, MA) (Roy 2008). Briefly, p53+/− progeny of p53−/− C57Bl/6 × SKH-1 hairless mouse was back-crossed with wild-type SKH-1 hairless mice for seven generations, until the p53+/− mice obtained displayed a phenotype of a typical SKH-1 hairless mouse. The genotype of the WT and p53+/− mice thus obtained was confirmed through PCR analysis. The DNA fragment for p53 gene was amplified using, sense oligonucleotide primer (5'-CCCGAGTATCTGGAAGACAG-3′) and an antisense primer (5′-ATAGGTCGGCGGTTCAT-3′), and the neomycin resistance gene insert cassette was amplified using sense oligonucleotide primer (5′-CTTGGGTGGAGAGGCTATTC-3′) and an antisense primer (5′-AGGTGAGATGACAGGAGATC-3′) (Matsusaka et al. 2006; Roy 2008). The PCR product from WT mice is 600 bp and p53+/− mice is 600 and 280 bp. Mice were housed under standard conditions, and all studies were carried out following approved IACUC protocol. Both WT and p53+/− SKH-1 hairless mice were exposed to 3.2 mg NM in 200 μL of acetone/mouse topically on to the dorsal skin for 24 and 72 h. Thereafter, mice were euthanized, and NM-exposed dorsal skin was collected and either snap frozen in liquid nitrogen or fixed in formalin for histology and immunohistochemical (IHC) analyses.

### 2.3 Western blot analysis

The skin tissues were cleaned to remove subcutaneous fat and whole skin tissue lysates were prepared as described earlier (Pal et al. 2009; Tewari-Singh et al. 2012). Protein content of the samples was determined by using the Lowry method, and 80 μg of protein per sample was denatured and resolved on SDS PAGE gels, and transferred on to a nitrocellulose membrane. The membrane was blocked in Odyssey blocking buffer for 1 h at room temperature and probed with p53 Ser15 antibody (Cell Signaling; Beverly, MA) overnight at 4°C followed by incubation with IRDye® 800CW conjugated Goat Anti-Rabbit IgG Polyclonal secondary antibody for 1 h at room temperature. The membrane was then visualized using Odyssey™ Infrared Imager (LI-COR Biosciences Lincoln, NE). To ensure equal protein loading, the membrane was stripped and reprobed with β-actin antibody (Sigma-Aldrich, St. Louis, MO).

### 2.4 Histopathological analysis, apoptotic cell death detection, and IHC staining

Formalin-fixed skin tissue samples were processed as reported earlier, and paraffin-embedded tissue blocks were used for 5 μm thick serial section preparation. Following

hematoxylin and eosin (H&E) staining, epidermal thickness (μm) and percentage dead epidermis were determined as described earlier (Jain et al. 2011b; Tewari-Singh et al. 2009). For dead epidermis measurement, we measured the total length of the epidermis in the skin section, and the same way we also measured the length of the areas where the epidermis was completely dead and then calculated the percentage dead epidermis. Apoptotic cell death was detected employing DeadEnd™ Colorimetric TUNEL assay and vendor's protocol as detailed earlier (Tewari-Singh et al. 2010). TUNEL positive cells were quantified in 15 randomly selected fields. IHC staining for macrophages was carried out using BM8 monoclonal F4/80 rat anti-mouse IgG2a antibody as described earlier (Tewari-Singh et al. 2009). Mast cells were detected by Toluidine blue staining as described previously (Tewari-Singh et al. 2009). Quantification for macrophage infiltration and mast cell population was done by counting positive-stained cells/$cm^2$ in five randomly-selected fields per section. All histopathology and IHC analyses were done using a Zeiss Axioscope 2 microscope (Carl Zeiss, Inc., Germany) equipped with Carl Zeiss AxioCam MrC5 camera at 400×, and images were processed using Axiovision Rel 4.5 software.

### 2.5 MPO activity assay

MPO assay was done employing Fluorescent Myeloperoxidase Detection Kit and vendor's protocol using 50 μg of protein/tissue sample as described previously (Tewari-Singh et al. 2009), and MPO activity was determined as mU/mL protein using MPO standard curve.

### 2.6 Statistical analysis

Statistical significance among different groups was determined by one-way ANOVA using SigmaStat 3.5 software (Jandel scientific, San Rafael, CA) and then Tukey test for multiple comparisons, with P-value of $< 0.05$ considered as significant.

## 3. Results

### 3.1 Effect of p53 deficiency on NM-induced epidermal thickness and % dead epidermis in SKH-1 hairless mouse skin

To study the effect of p53 heterozygosity on NM-induced p53 activation, we first carried out western blot analysis on control and NM exposed WT and p53+/− mouse skin. Our results showed that p53+/− mice demonstrated a significant decrease in NM-induced p53 Ser15 levels when compared to WT mice (Fig 1A). To further understand the consequences of NM exposure in skin deficient in functional p53, we microscopically examined the H&E stained skin sections for potential differences in epidermal thickness between WT and p53+/− mice. Our data showed that, compared to controls, 3.2 mg NM exposure for 24 h caused a significant increase in epidermal thickness in WT mice, but not in p53+/− mice (Fig 1B). Quantification of epidermal thickness in these mice showed that NM causes 63% increase in epidermal thickness after 24 h in WT mice. However, only a 25% increase in epidermal thickness was observed in p53+/− mice when compared to their respective controls (Fig 1C). A lack of NM effect on epidermal thickness was also evident in p53−/− SKH-1 hairless mice when compared to WT (Fig 1C). Since this lack of effect was consistent to that in case of p53+/− SKH-1 hairless mice (Fig 1C), we choose to continue our studies only with p53+/− mice. Our epidermal thickness measurements were limited to 24 h, as longer times (72 h) post NM exposure were associated with significant epidermal cell death in both WT and p53+/− mice (Fig 1D), making it impractical to measure epidermal thickness. Therefore, to quantify epidermal damage after 72 h, we measured the percentage of NM-induced dead epidermis. Microscopic evaluation of skin sections showed that control mice had no significant dead epidermis, as expected. However, both WT and p53+/− mice exposed to NM had large areas (~67%) of dead epidermis (Fig 1E).

### 3.2 Effect of p53 deficiency on NM-induced apoptotic cell death in SKH-1 hairless mouse skin

Apoptosis is one of the early homeostatic responses of damaged cells after mustard exposure, and p53 plays a major role in this process (Kan et al. 2003). Consequently, we quantified NM-induced apoptotic cell death. The representative pictures of TUNEL-stained skin sections in Fig 2 show that NM induced considerably greater apoptosis in WT mice relative to p53+/− mice (Fig 2A). Quantification of TUNEL-stained cells further confirmed this observation, where exposure of WT mice and p53+/− to NM resulted in 37 and 15% TUNEL-positive cells, respectively, in skin epidermis after 24 h compared to 3% in untreated controls (Fig 2B). Due to the significant amount of dead epidermis at 72 h after NM exposure (Fig 1C and 1D), apoptotic cells could not be identified at this later time point.

### 3.3 Effect of p53 deficiency on NM-induced inflammatory response in SKH-1 hairless mouse skin

Cell death by an external insult such as injury or infection invokes the innate immune response (Majno et al. 1960). This response includes an initial influx of neutrophils, followed by the influx of macrophages and mast cells (Chen et al. 2007). Based on our data showing that NM causes differential apoptotic cell death in epidermis at 24 h after exposure, we next measured the potential impact of this differential cell death on inflammation. First, we determined the infiltration of neutrophils in the skin by measuring MPO activity. NM exposure caused a 10.3-fold increase in MPO activity in WT mice compared to controls after 24 h, which persisted at 72 h after exposure. Importantly, exposure of p53+/− mice to NM resulted in only a 3.6-fold increase in MPO activity compared to controls after 24 h. However, in this case, MPO activity drastically increased to 13.6 fold at 72 h after exposure (Fig 3). We next employed IHC analysis to identify the infiltration of macrophages. F4/80 IHC staining of skin sections showed that NM exposure strongly increased the infiltration of macrophages in the dermis of WT mice, but not in p53+/− mice after 24 h (Fig. 4A). However, by 72 h of exposure, macrophage infiltration in the dermal region was greatly reduced in both WT and p53+/− mice when compared to control mice (Fig 4A). Quantification of macrophages further confirmed our observation, where 24 h after NM exposure there was a 2.7-fold increase in the number of macrophages in WT mouse dermis compared to control, but this effect disappeared by 72 h after exposure at which time few macrophages were present in NM-exposed mice relative to controls (Fig. 4B). On the other hand, NM exposure only minimally induced infiltration of macrophages in p53+/− mice after 24 h, which decreased to insignificant numbers compared to controls after 72 h of exposure (Fig 4B). Importantly, toluidine blue staining to identify mast cell infiltration also followed similar pattern, where at 24 h of NM exposure, a great influx of mast cells was evident in WT mice, which returned to basal levels by 72 h after exposure (Fig 4C). Conversely, NM did not induce any infiltration of mast cells after both 24 and 72 h after exposure in p53+/− mice relative to controls (Fig 4C). Quantification of mast cells further supported these observations in that 24 h after NM exposure there was a 2.7-fold increase in mast cell infiltration when compared to controls in WT mice, and this declined to control level by 72 h (Fig 4D). However, NM exposure did not induce any mast cell infiltration when compared to control in p53+/− mice at both 24 and 72 h after exposure (Fig 4D).

## 4. Discussion

Exposure of skin to NM/SM causes DNA damage and oxidative stress leading to cell death, which in turn contributes to skin injury, manifested mainly in the form of inflammation and vesication (Kehe et al. 2009). Though activation of p53 in response to SM/NM exposure has been widely reported (Inturi et al. 2011; Jowsey et al. 2012; Ruff and Dillman 2010; Tewari-Singh et al. 2012), its role in mustard-induced cell death and subsequent immune response

has not been elucidated. Identifying the role of p53 in the injury response to mustards could help inform therapeutic development toward agents that target p53 pathway and ameliorate injury. Employing SKH-1 hairless mice that were p53 sufficient (WT) or deficient (p53+/−), our findings demonstrated that p53 is an essential mediator of NM-induced apoptosis in mouse skin, and that p53 deficiency/decreased p53 activation significantly reduces early apoptotic cell death and neutrophilic infiltration induced by NM. Surprisingly, this reduced early apoptotic response in p53+/− mice (compared to wild-type) did not result in a difference in epidermal cell death between p53+/− and WT mice at 72 h after NM exposure. These results indicate that, even though the lack of p53 decreased early apoptotic epidermal cell death in p53+/− mice, late necrosis might not be affected by p53 status. It appears that the persistence of NM-induced DNA damage ultimately resulted in necrotic cell death. Whereas more studies are needed in the future to address this assumption, published reports have shown that apoptosis is one of the early mechanisms for clearance of injured cells, and this is followed by late necrosis through which nonviable cells are eliminated after exposure to mustards (Kan et al. 2003; Petrali et al. 1993).

Previous studies have shown that both apoptotic and necrotic cell death due to alkylating agents can trigger immune responses (Zong et al. 2004). In the event of cell death, various pro inflammatory mediators (TNF-α, IL-1α, IL-1β, IL-8, etc.,) are released into the extracellular matrix, activating the innate immune response including activation of resident macrophages and mast cells. These inflammatory cells further release proinflammatory mediators and chemo-attractants that function to activate extravasation and accumulation of neutrophils in the damaged area (Jaeschke 2006; Silva 2010). Following tissue infiltration, neutrophils generate chemotactic signals that attract monocytes and macrophages to the damaged area. These cells, depending on the status of the injury, could display a proinflammatory phenotype or help in wound repair. Such tissue repair involves phagocytizing apoptotic neutrophils, dead cells and debris at the site of injury, and through release of various growth factors which can help in advancing cell proliferation and the synthesis of extracellular matrix (Eming et al. 2007; Silva 2010). However, in case of persistent tissue stress, these cells could act as a source of proinflammatory mediators and cytokines, which could aid in further infiltration of neutrophils to the site of injury (Eming et al. 2007; Nathan 2006; Silva 2010). At the site of damage, neutrophils act through degranulation and release of MPO in to tissue microenvironment (Lefkowitz and Lefkowitz 2001). In the MPO assay, our results indicated an increase in neutrophil infiltration after 24 h of NM exposure in WT mice, which persisted through 72 h of exposure. The increase in neutrophils at 24 h after NM exposure also coincided with the increase in apoptotic cell death in WT mice. Thus, p53 activation may contribute to induction of initial inflammatory responses. The correlation between apoptotic cell death and neutrophil infiltration was also observed in p53+/− mice, where at 24 h after NM exposure, both MPO activity and apoptotic cell death were not significantly different from control mice. Importantly, by 72 h after NM exposure, a 13-fold increase in MPO levels in p53+/− mice also coincided with a marked increase in epidermal cell death, suggesting that cell death contributes to NM-induced skin inflammatory responses. The drastic increase in MPO levels in p53-deficient mice could be related to their p53 status; where absence of extensive apoptosis at 24 h in these mice prevented infiltration of neutrophils, but the persistence of the unrepaired epidermal cells ultimately led to necrosis, triggering a stronger neutrophil response relative to p53-sufficient mice.

The role of p53 in regulating mast cells and macrophages has been controversial. Earlier, p53 was shown to be a negative regulator of mast cells and macrophages and its absence caused their enhanced activation (Suzuki et al. 2011; Zheng et al. 2005). Conversely, p53 was also shown to enhance macrophage differentiation, with its mutation inhibiting macrophage differentiation (Matas et al. 2004). Employing p53+/− rat model, Yan et al.

showed that in response to DNA damage due to diethylnitrosamine, p53+/− rats had decreased infiltration of inflammatory cells when compared to WT rats (Yan et al. 2012). Similarly, in our present study, NM exposure for 24 h caused nearly 3-fold increase in macrophage and mast cell infiltration in WT mice, but no increase was observed in p53+/− mice. Also notably, the levels of these inflammatory cells were comparable in both control WT and p53+/− mice, but NM exposure failed to induce their further infiltration in p53+/− mice. This suggested that p53 deficiency did not affect differentiation of these inflammatory cells, but influenced the signals that trigger their infiltration following NM exposure.

Whereas additional studies are needed in future to further address the above-mentioned assumptions, our results clearly show that p53 deficiency causes a delay in NM-induced early apoptosis and inflammatory response, which could be exploited in developing new therapies to prevent or treat mustard-induced skin injuries.

## Acknowledgments

This work was supported by the Countermeasures Against Chemical Threats (CounterACT) Program, National Institutes of Health Office of the Director, and the National Institute of Environmental Health Sciences, [Grant U54ES-015678]. The study sponsors have no involvement in the study design; collection, analysis and interpretation of data; the writing of the manuscript; and the decision to submit the manuscript for publication.

## List of Abbreviations

| | |
|---|---|
| **ATM** | Ataxia telangiectasia mutated |
| **ATR** | Ataxia telangiectasia-Rad3-related |
| **CEES** | 2-chloroethyl ethyl sulfide |
| **GSH** | Glutathione |
| **MPO** | Myeloperoxidase |
| **NM** | Nitrogen mustard |
| **PARP** | Poly (ADP-ribose) polymerase |
| **p53+/−** | p53 heterozygous |
| **p53−/−** | p53 knock out |
| **SM** | Sulfur mustard |
| **TUNEL** | TdT-mediated dUTP Nick-End Labeling |
| **WT** | p53 wild type |

## References

Atkinson WS. Delayed Mustard Gas Keratitis (Dichlorodiethyl Sulfide). A Report of Two Cases. Trans Am Ophthalmol Soc. 1947; 45:81–92. [PubMed: 16693466]

Basu S, Binder RJ, Suto R, Anderson KM, Srivastava PK. Necrotic but not apoptotic cell death releases heat shock proteins, which deliver a partial maturation signal to dendritic cells and activate the NF-kappa B pathway. International immunology. 2000; 12:1539–1546. [PubMed: 11058573]

Boley SE, Wong VA, French JE, Recio L. p53 heterozygosity alters the mRNA expression of p53 target genes in the bone marrow in response to inhaled benzene. Toxicol Sci. 2002; 66:209–215. [PubMed: 11896287]

Chen CJ, Kono H, Golenbock D, Reed G, Akira S, Rock KL. Identification of a key pathway required for the sterile inflammatory response triggered by dying cells. Nature medicine. 2007; 13:851–856.

Chilcott RP, Jenner J, Carrick W, Hotchkiss SA, Rice P. Human skin absorption of Bis-2-(chloroethyl)sulphide (sulphur mustard) in vitro. J Appl Toxicol. 2000; 20:349–355. [PubMed: 11139165]

Dirven HA, van Ommen B, van Bladeren PJ. Glutathione conjugation of alkylating cytostatic drugs with a nitrogen mustard group and the role of glutathione S-transferases. Chem Res Toxicol. 1996; 9:351–360. [PubMed: 8839035]

Eming SA, Krieg T, Davidson JM. Inflammation in wound repair: molecular and cellular mechanisms. J Invest Dermatol. 2007; 127:514–525. [PubMed: 17299434]

Ghanei M, Poursaleh Z, Harandi AA, Emadi SE, Emadi SN. Acute and chronic effects of sulfur mustard on the skin: a comprehensive review. Cutan Ocul Toxicol. 2010; 29:269–277. [PubMed: 20868209]

Gu M, Singh RP, Dhanalakshmi S, Agarwal C, Agarwal R. Silibinin inhibits inflammatory and angiogenic attributes in photocarcinogenesis in SKH-1 hairless mice. Cancer Res. 2007; 67:3483–3491. [PubMed: 17409458]

Guainazzi A, Campbell AJ, Angelov T, Simmerling C, Scharer OD. Synthesis and molecular modeling of a nitrogen mustard DNA interstrand crosslink. Chemistry. 2010; 16:12100–12103. [PubMed: 20842675]

Haupt S, Berger M, Goldberg Z, Haupt Y. Apoptosis - the p53 network. Journal of cell science. 2003; 116:4077–4085. [PubMed: 12972501]

Hawkins DS, Demers GW, Galloway DA. Inactivation of p53 enhances sensitivity to multiple chemotherapeutic agents. Cancer Res. 1996; 56:892–898. [PubMed: 8631030]

Ikehata H, Okuyama R, Ogawa E, Nakamura S, Usami A, Mori T, Tanaka K, Aiba S, Ono T. Influences of p53 deficiency on the apoptotic response, DNA damage removal and mutagenesis in UVB-exposed mouse skin. Mutagenesis. 2010; 25:397–405. [PubMed: 20462948]

Inturi S, Tewari-Singh N, Gu M, Shrotriya S, Gomez J, Agarwal C, White CW, Agarwal R. Mechanisms of sulfur mustard analog 2-chloroethyl ethyl sulfide-induced DNA damage in skin epidermal cells and fibroblasts. Free Radic Biol Med. 2011; 51:2272–2280. [PubMed: 21920433]

Jaeschke H. Mechanisms of Liver Injury. II. Mechanisms of neutrophil-induced liver cell injury during hepatic ischemia-reperfusion and other acute inflammatory conditions. American journal of physiology. Gastrointestinal and liver physiology. 2006; 290:G1083–G1088. [PubMed: 16687579]

Jain AK, Tewari-Singh N, Gu M, Inturi S, White CW, Agarwal R. Sulfur mustard analog 2-chloroethyl ethyl sulfide-induced skin injury involves DNA damage and induction of inflammatory mediators, in part via oxidative stress, in SKH-1 hairless mouse skin. Toxicol Lett. 2011a; 205:293–301. [PubMed: 21722719]

Jain AK, Tewari-Singh N, Orlicky DJ, White CW, Agarwal R. 2-Chloroethyl ethyl sulfide causes microvesication and inflammation-related histopathological changes in male hairless mouse skin. Toxicology. 2011b; 282:129–138. [PubMed: 21295104]

Joseph LB, Gerecke DR, Heck DE, Black AT, Sinko PJ, Cervelli JA, Casillas RP, Babin MC, Laskin DL, Laskin JD. Structural changes in the skin of hairless mice following exposure to sulfur mustard correlate with inflammation and DNA damage. Experimental and molecular pathology. 2011; 91:515–527. [PubMed: 21672537]

Jowsey PA, Williams FM, Blain PG. DNA damage responses in cells exposed to sulphur mustard. Toxicol Lett. 2012; 209:1–10. [PubMed: 22119920]

Kan RK, Pleva CM, Hamilton TA, Anderson DR, Petrali JP. Sulfur mustard-induced apoptosis in hairless guinea pig skin. Toxicologic pathology. 2003; 31:185–190. [PubMed: 12696578]

Kehe K, Balszuweit F, Emmler J, Kreppel H, Jochum M, Thiermann H. Sulfur mustard research--strategies for the development of improved medical therapy. Eplasty. 2008; 8:e32. [PubMed: 18615149]

Kehe K, Balszuweit F, Steinritz D, Thiermann H. Molecular toxicology of sulfur mustard-induced cutaneous inflammation and blistering. Toxicology. 2009; 263:12–19. [PubMed: 19651324]

Kono H, Rock KL. How dying cells alert the immune system to danger. Nature reviews. Immunology. 2008; 8:279–289. [PubMed: 18340345]

Kumar P, Gautam A, Prakash CJ, Kumar A, Ganeshan K, Pathak U, Vijayaraghavan R. Ameliorative effect of DRDE 07 and its analogues on the systemic toxicity of sulphur mustard and nitrogen mustard in rabbit. Hum Exp Toxicol. 2010; 29:747–755. [PubMed: 20164158]

Lane DP. Cancer. p53, guardian of the genome. Nature. 1992; 358:15–16. [PubMed: 1614522]

Lavin MF, Kozlov S. ATM activation and DNA damage response. Cell Cycle. 2007; 6:931–942. [PubMed: 17457059]

Le HQ, Knudsen SJ. Exposure to a First World War blistering agent. Emerg Med J. 2006; 23:296–299. [PubMed: 16549577]

Lefkowitz DL, Lefkowitz SS. Macrophage-neutrophil interaction: a paradigm for chronic inflammation revisited. Immunology and cell biology. 2001; 79:502–506. [PubMed: 11564158]

Majno G, La Gattuta M, Thompson TE. Cellular death and necrosis: chemical, physical and morphologic changes in rat liver. Virchows Archiv fur pathologische Anatomie und Physiologie und fur klinische Medizin. 1960; 333:421–465. [PubMed: 13765553]

Matas D, Milyavsky M, Shats I, Nissim L, Goldfinger N, Rotter V. p53 is a regulator of macrophage differentiation. Cell Death Differ. 2004; 11:458–467. [PubMed: 14713961]

Matsusaka H, Ide T, Matsushima S, Ikeuchi M, Kubota T, Sunagawa K, Kinugawa S, Tsutsui H. Targeted deletion of p53 prevents cardiac rupture after myocardial infarction in mice. Cardiovasc Res. 2006; 70:457–465. [PubMed: 16533502]

Minsavage GD, Dillman JF 3rd. Bifunctional alkylating agent-induced p53 and nonclassical nuclear factor kappaB responses and cell death are altered by caffeic acid phenethyl ester: a potential role for antioxidant/electrophilic response-element signaling. J Pharmacol Exp Ther. 2007; 321:202–212. [PubMed: 17204746]

Nathan C. Neutrophils and immunity: challenges and opportunities. Nature reviews. Immunology. 2006; 6:173–182. [PubMed: 16498448]

Newmark J, Langer JM, Capacio B, Barr J, McIntosh RG. Liquid sulfur mustard exposure. Mil Med. 2007; 172:196–198. [PubMed: 17357776]

Pal A, Tewari-Singh N, Gu M, Agarwal C, Huang J, Day BJ, White CW, Agarwal R. Sulfur mustard analog induces oxidative stress and activates signaling cascades in the skin of SKH-1 hairless mice. Free Radic Biol Med. 2009; 47:1640–1651. [PubMed: 19761830]

Papirmeister B, Gross CL, Petrali JP, Meier HL. Pathology Produced by Sulfur Mustard in Human Skin Grafts on Athymic Nude Mice. II. Ultrastructural Changes. Cutaneous and Ocular Toxicology. 1984; 3:393–408.

Paromov V, Suntres Z, Smith M, Stone WL. Sulfur mustard toxicity following dermal exposure: role of oxidative stress, and antioxidant therapy. J Burns Wounds. 2007; 7:e7. [PubMed: 18091984]

Petrali JP, Oglesby SB, Hamilton TA, Mills KR. Comparative morphology of sulfur mustard effects in the hairless guinea pig and a human skin equivalent. J Submicrosc Cytol Pathol. 1993; 25:113–118. [PubMed: 8462065]

Rock KL, Kono H. The inflammatory response to cell death. Annual review of pathology. 2008; 3:99–126.

Roy, S. Defining the Mechanism of Action of Silibinin as an Anti-cancer and Cancer Chemopreventive Agent. Department of Pharmaceutical Sciences, University of Colorado Health Sciences Center; 2008.

Ruff AL, Dillman JF 3rd. Sulfur mustard induced cytokine production and cell death: investigating the potential roles of the p38, p53, and NF-kappaB signaling pathways with RNA interference. J Biochem Mol Toxicol. 2010; 24:155–164. [PubMed: 20143454]

Rutman RJ, Chun EH, Jones J. Observations on the mechanism of the alkylation reaction between nitrogen mustard and DNA. Biochim Biophys Acta. 1969; 174:663–673. [PubMed: 5813318]

Shakarjian MP, Heck DE, Gray JP, Sinko PJ, Gordon MK, Casillas RP, Heindel ND, Gerecke DR, Laskin DL, Laskin JD. Mechanisms mediating the vesicant actions of sulfur mustard after cutaneous exposure. Toxicol Sci. 2010; 114:5–19. [PubMed: 19833738]

Sharma M, Vijayaraghavan R, Ganesan K. Comparison of toxicity of selected mustard agents by percutaneous and subcutaneous routes. Indian J Exp Biol. 2008; 46:822–830. [PubMed: 19245179]

Shi Y, Zheng W, Rock KL. Cell injury releases endogenous adjuvants that stimulate cytotoxic T cell responses. Proc Natl Acad Sci U S A. 2000; 97:14590–14595. [PubMed: 11106387]

Shukla PK, Mishra PC, Suhai S. Reactions of DNA bases with the anti-cancer nitrogen mustard mechlorethamine: A quantum chemical study. Chemical Physics Letters. 2007; 449:323–328.

Silva MT. When two is better than one: macrophages and neutrophils work in concert in innate immunity as complementary and cooperative partners of a myeloid phagocyte system. J Leukoc Biol. 2010; 87:93–106. [PubMed: 20052802]

Suzuki K, Murphy SH, Xia Y, Yokota M, Nakagomi D, Liu F, Verma IM, Nakajima H. Tumor suppressor p53 functions as a negative regulator in IgE-mediated mast cell activation. PLoS One. 2011; 6:e25412. [PubMed: 21966524]

Tavana O, Benjamin CL, Puebla-Osorio N, Sang M, Ullrich SE, Ananthaswamy HN, Zhu C. Absence of p53-dependent apoptosis leads to UV radiation hypersensitivity, enhanced immunosuppression and cellular senescence. Cell Cycle. 2010; 9:3328–3336. [PubMed: 20703098]

Tewari-Singh N, Gu M, Agarwal C, White CW, Agarwal R. Biological and molecular mechanisms of sulfur mustard analogue-induced toxicity in JB6 and HaCaT cells: possible role of ataxia telangiectasia-mutated/ataxia telangiectasia-Rad3-related cell cycle checkpoint pathway. Chem Res Toxicol. 2010; 23:1034–1044. [PubMed: 20469912]

Tewari-Singh N, Jain AK, Inturi S, Agarwal C, White CW, Agarwal R. Silibinin attenuates sulfur mustard analog-induced skin injury by targeting multiple pathways connecting oxidative stress and inflammation. PLoS One. 2012; 7:e46149. [PubMed: 23029417]

Tewari-Singh N, Rana S, Gu M, Pal A, Orlicky DJ, White CW, Agarwal R. Inflammatory biomarkers of sulfur mustard analog 2-chloroethyl ethyl sulfide-induced skin injury in SKH-1 hairless mice. Toxicol Sci. 2009; 108:194–206. [PubMed: 19075041]

Yan HX, Wu HP, Zhang HL, Ashton C, Tong C, Wu J, Qian QJ, Wang HY, Ying QL. DNA damage-induced sustained p53 activation contributes to inflammation-associated hepatocarcinogenesis in rats. Oncogene. 2012

Zheng SJ, Lamhamedi-Cherradi SE, Wang P, Xu L, Chen YH. Tumor suppressor p53 inhibits autoimmune inflammation and macrophage function. Diabetes. 2005; 54:1423–1428. [PubMed: 15855329]

Zong WX, Ditsworth D, Bauer DE, Wang ZQ, Thompson CB. Alkylating DNA damage stimulates a regulated form of necrotic cell death. Genes & development. 2004; 18:1272–1282. [PubMed: 15145826]

- P53 deficiency caused a delay in NM-induced early apoptosis in mouse skin epidermis.
- P53 deficiency caused a delay in neutrophil infiltration in NM exposed mouse skin.
- Cell death at 72 h of NM exposure increased neutrophil infiltration in p53+/− mice.
- NM-induced macrophage and mast cell infiltration was prevented in p53+/− mice.

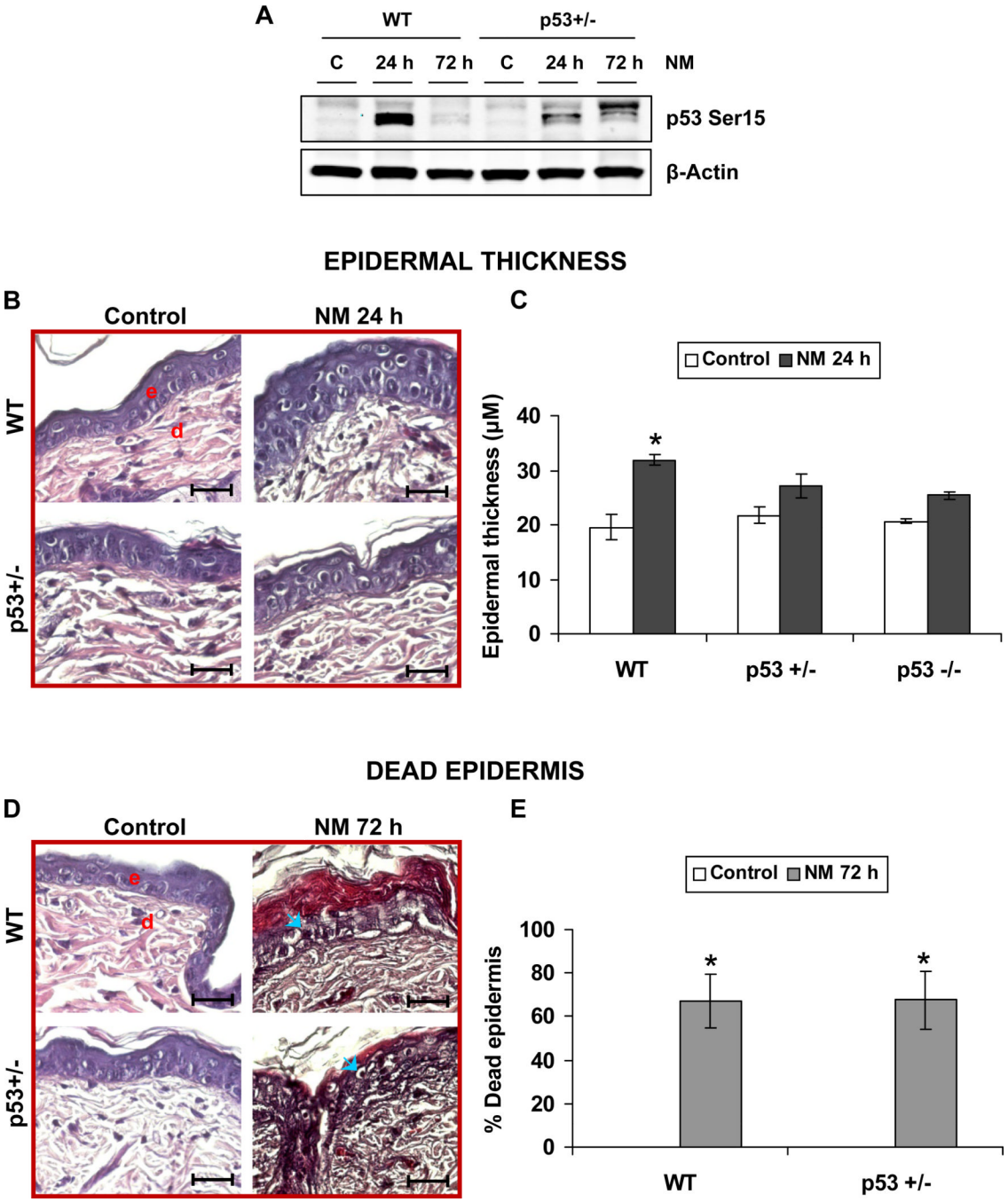


**Figure 1. Effect of p53 on NM-induced epidermal thickness and percentage dead epidermis**

Dorsal skin of WT and p53+/− and p53−/− SKH-1 hairless mice was exposed topically to 3.2 mg NM for 24 and 72 h. Thereafter, mice were sacrificed and skin tissues were collected and processed as detailed under material and methods. Whole cell lysates were prepared from the skin and subjected to western immunoblot analysis for p53 Ser15 as detailed under Materials and Methods (A). Protein loading was determined by stripping and reprobing the membrane with β-Actin antibody (A). 5μm thick skin sections were processed for H&E staining and analyzed for epidermal thickness and percentage dead epidermis. Epidermal thickness after 24 h of NM exposure is shown in representative pictures (B), which was quantified (C) as detailed in materials and methods. Percentage dead epidermis shown in

representative pictures (D) was quantified at 72 h of NM exposure (E). Data are presented as mean ± SEM of four animals in NM-exposed groups and three in respective controls. *, $p < 0.05$ as compared to controls. e, epidermis; d, dermis; blue arrows, dead epidermis. Black scale bar = 100 μm.

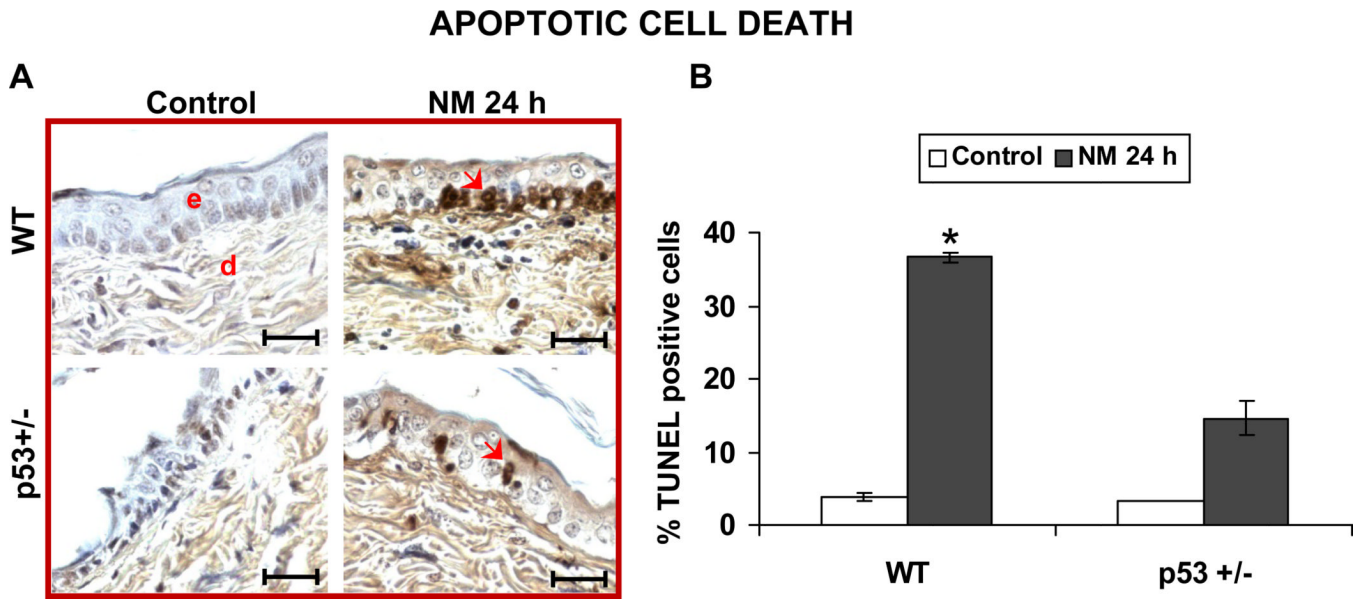


**Figure 2. Effect of p53 on NM-induced apoptotic epidermal cell death**

Skin sections from the study detailed in Figure 1 legend, were processed for TUNEL staining to determine apoptotic cell death as shown in representative pictures (A). Percent TUNEL positive cells were quantified by counting positive stained cells and the total number of cells in fifteen randomly selected fields per slide at 400× magnification as described under materials and methods. Data are presented as mean ± SEM of four animals in NM-exposed groups and three in respective controls. *, $p < 0.05$ as compared to controls. e, epidermis; d, dermis; Red arrows indicate TUNEL positive cells. Black scale bar = 100 μm.

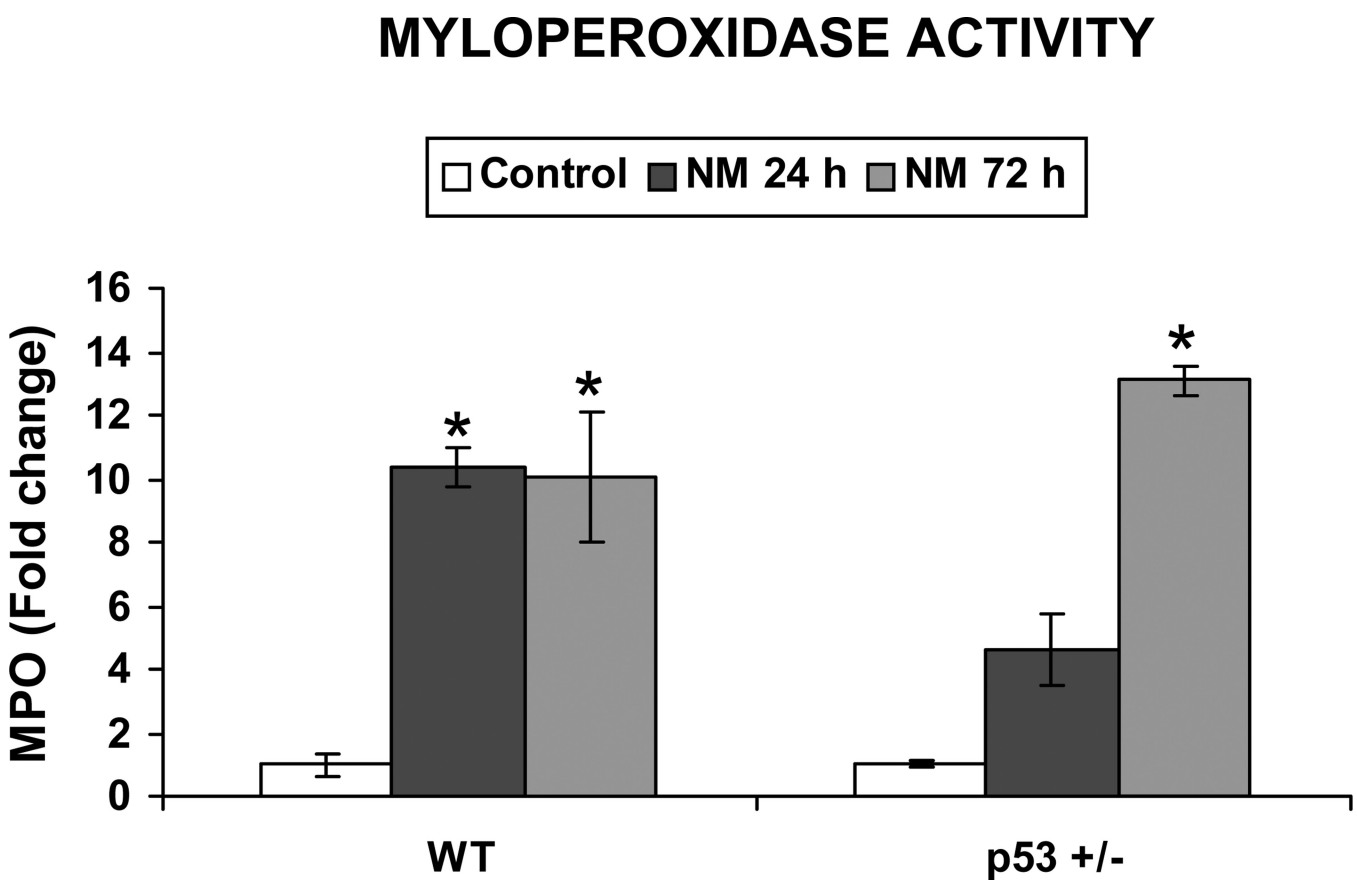


**Figure 3. Effect of p53 on NM-induced neutrophil infiltration**

Skin tissue samples from the study detailed in Figure 1 legend were employed for lysate preparation and MPO activity was measured as detailed in materials and methods. Data are presented as mean ± SEM of four animals in NM-exposed groups and three in respective controls. *, $p < 0.05$ as compared to controls.

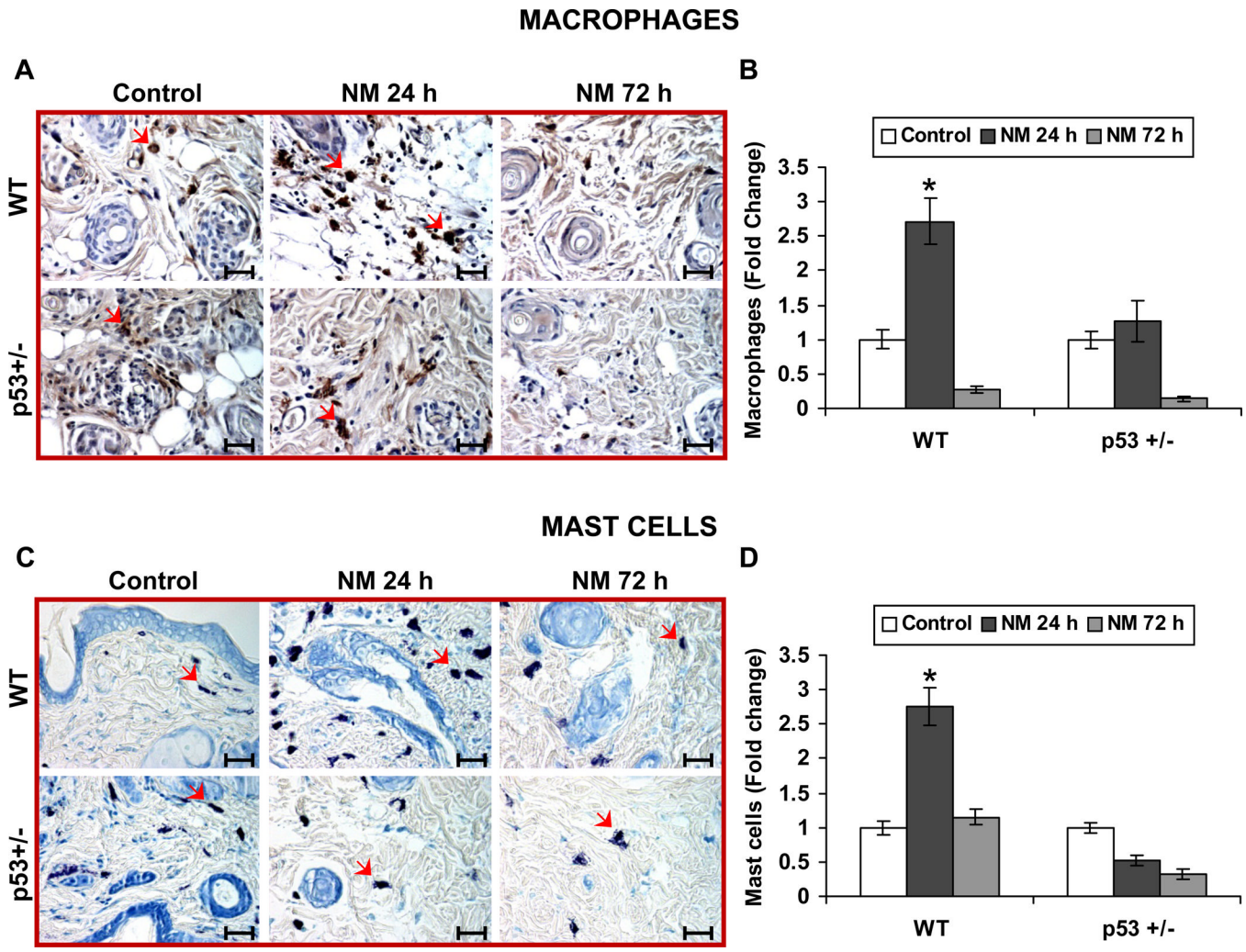


**Figure 4. Effect of p53 on NM-induced inflammatory responses**

Skin sections from the study detailed in Figure 1 legend, were stained for macrophages and mast cells as detailed in materials and methods. Representative pictures (A) show F4/80 IHC staining for macrophages, which were quantified (B). Mast cells were identified by toluidine blue staining as shown in representative pictures (C) and quantified (D). Data are presented as mean ± SEM of four animals in NM-exposed groups and three in respective controls. *, $p < 0.05$ as compared to controls. Red arrows, macrophages in 'A' and mast cells in 'C'. Black scale bar = 100 μm.